Supporting Information

Pernthaler *et al.* 10.1073/pnas.0711303105

SI Text

Site Selection and Sampling. Methane seep sediments analyzed in this study were collected from active methane seeps at 520 m water depth in the Eel River Basin off the coast of Northern California (for description, see ref. 1). Deep-sea sediment samples were collected by push core in October 2006 using the manned submersible *Alvin.* A 30-cm push core (PC-29), collected through a habitat transition zone consisting of sulfide oxidizing microbial mat and some chemosynthetic clams was selected for further analysis in this study. Core processing was completed shipboard as described in Orphan *et al.* (2). From the push core sleeve, samples were extruded upwards and subsampled by using cut-off 5cc syringes. Samples for microscopy were preserved shipboard for ≈10 h at 4°C in phosphate-buffered 2% paraformaldehyde, rinsed twice with 1× PBS (PBS). After fixation, samples were flash frozen in liquid nitrogen and stored at −80°C. Upon arrival in the lab, samples were thawed at room temperature (RT), washed in 1× PBS [145 mM NaCl, 1.4 mM NaH_2PO_4, 8 mM Na_2HPO_4 (pH 7.4)], then in 1× PBS and 50% ethanol, resuspended in 100% ethanol and stored at −80°C until further processing. Fixed sediments from the 3- to 6-cm depth horizon were used for the ANME-2c Magneto-FISH capture.

PCR and Cloning of 16S rRNA and Metabolic Genes (nifH). Archaeal and bacterial 16S rRNA diversity was assessed before and after the ANME-2c capture using a DNA sample extracted from the bulk sediment (PC29, 3–6 cm) and DNA recovered from the bead-captured assemblage. Archaeal 16S rRNA genes were amplified by using *Archaea*-specific 16S rRNA primers, 20F and 958R (3). Bacterial 16S rRNA genes were amplified by using the *Bacteria*-specific 16S rRNA primer, 27F and the universal primer 1492R (4). Thermal cycling conditions included 1 min each of denaturation at 94°C, annealing at 54°C and elongation (72°C) for 30 cycles, and a 10-min final extension (72°C). The *nifH* gene was amplified from both the captured DNA and additional methane seep sediment samples from the Eel River Basin using the primers nifHf-10aa and nifHr-132aa reported by ref. 5. Amplification conditions included 30 sec of denaturation at 94°C, 30 sec of annealing at 58°C, and 1 min elongation at 72°C for 35 cycles followed by 10 min final elongation step at 72°C. All PCR reactions were conducted by using positive and negative (no template) controls in 25-μl total volume containing 0.4 μM final of forward and reverse primer, 1× Hot Master TaqPCR buffer (Qiagen), 0.2 mM dNTPs, and 0.2U of Hot master TaqDNA Polymerase (Qiagen). PCR amplicons were pooled from three reactions and cleaned by using a MultiScreen PCR Plate (Millipore). Cleaned 16S rRNA PCR products from both archaea and bacteria were cloned with a pCR 4.0 TOPO TA cloning kit according to the instructions of the manufacturer (Invitrogen). *Nif*H genes were cloned with a pGEM-T cloning kit according to the instructions of the manufacturer (Promega). To group similar clone types for subsequent sequence analysis, archaeal and bacterial 16S rRNA and *nifH* clone libraries were screened with restriction fragment length polymorphism (RFLP) analysis on M13F- and M13R-amplified products using RsaI, HaeIII or a mix of MaeII and HhaI (New England Biolabs) following the protocol outlined in ref. 2. Briefly, 2–4 μl of the PCR product was digested with 0.5 μl of restriction enzyme and 2 μl of buffer in a 20-μl total volume, in a histological microwave oven (Microwave Research & Applications) at 37°C for 10 min. One to three representative clones displaying unique restriction patterns were cleaned before sequencing with MultiScreen HTS plates (Millipore). Sequencing reactions were performed on the M13 amplified products using Genome Lab DTCS Quick Start Kit, then precipitated with glycogen and sodium acetate added as carriers, resuspended in 40 μl of formamide, and run on a CEQ 8800 Genetic Analysis System (Beckman Coulter).

Sequential Fluorescence *in Situ* Hybridization with CARD-FISH. To illustrate associations between microbes detected in sequence data, we used probes specific to ANME-2c [ANME2c_760 (6)], *Desulfosarcina* [DSS_225 (7)], *Desulfobulbus* [DBB_660 (8)], ANME2 [ANME2_932 (9)], *Desulfobacteriaceae* [DSS_658 (10)], α-proteobacteria [ALF_968 (11)], and β-proteobacteria [BET_42a (12)]. All probes were labeled with a horseradish peroxidase (Biomers). For multiple fluorescence *in situ* hybridizations, sediment was spotted onto glass slides (SuperFrost Plus; Fisher Scientific), air dried, covered with 0.1% agarose in sterile de-ionized water, air dried again, and dehydrated with absolute ethanol for 2 to 5 min. The dried slides were then covered with 300 μl of hybridization buffer (Formamide concentrations where: 60% for DSS_658, 20% for ANME_932, 35% for Bet_42a and ALF_968, 50% for ANME2c_760, 30% for DSS_225, and 15% for DSB_660) and 0.17 ng·μl^{-1} of horseradish peroxidase labeled oligonucleotide probe and a coverslip and hybridized at 46°C in a microwave oven for 20 min. After hybridization, the slides were washed in 1× PBS [137 mM NaCl, 2.7 mM KCl, 10 mM Na_2HPO_4, and 2 mM KH_2PO_4 (pH 7.6)]. Catalyzed reporter deposition, using the fluorochromes Alexa Fluor 546, Alexa Fluor 488, and Alexa Fluor 633, was carried out in series as described in ref. 13. Micrograph images were taken with a Deltavision RT microscope system (Applied Precision) equipped with a HBO 100-W Hg vapor lamp, appropriate filter sets for Cy3/Alexa Fluor 546, fluorescein/Alexa Fluor 488, Cy5/Alexa Fluor 633, and DAPI fluorescence and a 60× Olympus objective.

Magnetic Separation of Paramagnetic Beads and Associated Microorganisms. To obtain a pure fraction of hybridized target cells free from sediment particles and unlabeled cells, an apparatus consisting of two separation funnels was used (Fig. S1*g*). Here, funnel A is filled with 125 ml of 1× PBS buffer. After incubation with paramagnetic beads, the sediment slurry is gently pipetted into funnel A, and cells captured by the paramagnetic beads are concentrated at the top of funnel A with a strong Neodymium ring magnet, whereas nonmagnetic residue consisting of nonhybridized cells and sediment are separated by gravity. To gently wash away residual particulates adhering to the paramagnetic beads, a second funnel (B), is filled with 250 ml of 1× PBS is seated on top of funnel A. The valves of both funnels are then opened to let PBS flow slowly from B to A, while the captured cells on the ring magnet are always immersed in PBS, preventing disturbance and loss of the target cells that we observed when the bead-cell complex had air contact. To maximize yield, non-captured cells and sediment particles that were washed out during this procedure were again concentrated by centrifugation and incubated with fresh paramagnetic beads as described above. In the last step, funnel B is disconnected from funnel A and the PBS is drained so that the captured cells are now above the PBS level. To remove nonhybridized cells and particles adhered to the glass surface, the lower half of funnel A was rinsed repeatedly with PBS while the magnet was still applied. To recover the paramagnetic beads and captured cells, the magnet was re-

moved, the funnel tilted, and the captured cells were resuspended in a small volume of 1× TE (0.5 ml), and drained through the top opening of funnel A. A second wash step with 0.5 ml of 1× TE was used to recover remaining cells in funnel A and pooled with the first.

We note that a similar method using polyribonucleotide probes has shown some success in controlled mixed culture experiments (14); however, magneto-FISH is the first successful demonstration of a culture-independent magnetic cell capture and genomic analysis of target microorganisms from complex natural environments.

DNA Extraction. The captured cells were incubated in a lysis solution [1 ml of Tris/EDTA buffer (pH 9.0) containing 1% SDS and 2 mg·ml^{-1} of proteinase K] at 52°C for 2 h. The DNA was then extracted with Phenol-Chloroform-Isoamylalcohol, precipitated, and resuspended in 10 μl of MQwater. DNA extraction from PC29 bulk sediment from the same 3- to 6-cm depth interval (≈0.5 g of wet weight) was conducted by using the MoBio Ultraclean soil kit following the protocol of Orphan *et al.* (2).

DNA Amplification with Multiple Displacement Amplification (MDA). Captured DNA template (1–2 μl) was subjected to multiple displacement amplification (MDA), using a commercial kit (GenomiPhi; GE Healthcare), following the manufacturer's instructions (overnight incubation at 30°C). The amplified DNA was precipitated by using 0.5 M ammonium acetate and 95% ethanol for 3 h at −80°C, pelleted by centrifugation at 16,000 × *g* for 20 min at 4°C and rinsed twice with ice-cold absolute ethanol and once with cold 70% ethanol. The pellet was then resuspended in 20 μl of MQ water and stored in aliquots at −20°C. Amplified DNA (2 μl) was run on a 0.8% agarose gel, stained with SybrGold, and viewed on a UV transilluminator (Fig. S2).

Pyrosequencing and Bioinformatics Analysis. Sequencing of the MDA amplified DNA from the bead captured ANME-2c consortia was accomplished by clone free pyrosequencing (454 Life Sciences). Library preparation was conducted at 454 Life Sciences, and a single plate was analyzed by using the Genome Sequencer 20 System.

Trace Statistics and Cleanup. A total of 290,073 traces, containing 259,091 unique sequences, were obtained by pyrosequencing as described above with an average length of 99 bp. More than 3,900 of these sequences contained "Ns", which is a signature of low-quality 454 sequence reads (15). We also found that ≈8,500 distinct traces contained subsequences represented in at least 250 other traces, as measured by blastn bit scores >50. These over-represented subsequences do not represent amplification bias or read error because they are not clonal, but rather are probably repetitive genomic elements that could skew later protein homology searches. We therefore decided to remove them from the sequence collection. After removing the traces with repetitive subsequences, duplicate traces, and traces containing Ns, the sequence collection contained 246,703 traces with an average length of 98.7 bp. All further analyses were done on these remaining traces.

Trace Matching and Classification. Homologies to known proteins (National Center for Biotechnology Information nr database) and environmental sequences (National Center for Biotechnology Information env_nr database) were computed by reciprocal BLAST (tblastn and blastx) with an expectation cutoff of 1e-3. Putative protein orthologies were assigned by further restricting matches to the best reciprocal match; when there were multiple (equivalent) best matches, all matching proteins were tallied as putative orthologs. A tentative phylogenetic classification of traces was made with a MEGAN-style analysis where the taxonomic node assigned to a trace was the shallowest taxonomic node to which all protein homologs were assigned (16). Applying these criteria, reciprocal BLAST searches resulted in 38,242 matches to putative protein coding genes, representing 15.5% of the sequence reads, in line with reports from other environmental metagenomic studies (17).

Fosmid Coverage Calculations. To assess the extent of overlap between the metagenomic sequences and previously sequenced fosmids from the Eel River Basin (Fig. S4) (18), we assigned traces to fosmids with BLAST using an expectation cutoff of 1×10^{-3}. Coverage statistics were calculated by flattening all matching traces onto the fosmid sequence and counting covered vs. uncovered bases. In total, blast analysis against 230 kb of fosmid data resulted in an estimated 23% coverage at 1× or better. Verified ANME-2c fosmids (containing 16S rRNA or methyl coenzyme M reductase, mcrA) yielded a higher percentage of homologous gene fragments (24–35%) compared to identified ANME-1 fosmids (2–3%).

Protein Coverage Calculations. Homologies and putative orthologies to specific protein coding datasets from microbial genomes were calculated by using reciprocal BLAST between the trace database and the protein coding datasets (Table S1). An expectation cutoff of 1×10^{-3} was used in all BLASTs. Putative orthology numbers were calculated by assigning each trace to a reciprocal best BLAST hit with a protein sequence, thus assigning at most one trace to each protein in a genome, and homology numbers were calculated from all reciprocal matches between a trace and a protein. Our orthology criteria are intentionally strict and underestimate the true protein coverage, while the homology numbers slightly overestimate the true protein coverage.

Software Availability. All software for trace statistics, BLAST parsing, sequence extraction, and taxonomy classification was written in Python and run under Linux. It is open source and available upon request. The *blaster* software for calculating coverage numbers is written in Python and is also available upon request.

$^{15}N_2$ Sediment Incubation and FISH-SIMS Analysis. Methane seep sediment was collected from the Southern Ridge of Eel River Basin (40 47.1919; 124 35.7057). Sediments overlain by a sulfide-oxidizing microbial mat (PC-14) were stored at 4°C in a sealed container under argon. Before transfer into individual incubation bottles for the ^{15}N experiments, sediments from PC-14 were combined from different depths (1–13 cm), mixed (1:1) with anoxic-filtered 500 ml of water from Eel River Basin and stored at 4°C in a gas tight container under a methane headspace for 7 weeks. Bottles actively producing sulfide (a proxy for AOM activity) were used in the ^{15}N incubation experiments. An aliquot of this sediment was washed and mixed (1:1) with sterilized anoxic marine media (19), modified from by removing all sources of nitrogen. Thirty-five milliliters of slurry were transferred to anaerobic 120-ml serum bottles in triplicate. A headspace of ≈5% $^{15}N_2$ (99.8%); (Cambridge Isotope Laboratories) in methane was added to a final pressure of 2 atm. Sediment slurries were incubated at 8°C in the dark for 6 months. The duration of the incubation was chosen to allow for ≈1–2 doublings of the methane-oxidizing ANME/DSS consortia (see text). At the 6-month time point, an aliquot of slurry was sampled by using a sterile airtight syringe. Sampled sediment was fixed with 2% formaldehyde in PBS at room temperature for one hour, then washed with PBS, PBS:EtOH (1:1) and EtOH (100%). Samples for FISH-SIMS were prepared on 1-inch glass rounds according to (20). A general archaeal probe Arch 915 and bacterial probe

Eub 338 (3 mix) were used with a FISH hybridization buffer containing 35% formamide. Subsequent hybridizations using ANME-specific Eel 932 and DSS-specific DSS 658 demonstrated the $^{15}N_2$ incubation was dominated by ANME-2/DSS consortia, and yielded near identical percentages of total DAPI stained cell aggregates using either the general archaeal/bacterial probes or specific probes targeting the ANME-2/DSS. The dominance of ANME-2 and DSS aggregates observed in the incubation, combined with the characteristic $\delta^{13}C$ depletion in biomass (Fig. 4), is a strong indication that the aggregates analyzed by SIMS were composed of methanotrophic ANME-2 and DSS.

Combined carbon and nitrogen isotopic compositions of individual layered archaeal bacterial aggregates identified by FISH were measured by using the UCLA CAMECA ims 1270 ion microprobe using a $\approx$10-μm Cs^+ ion beam. The carbon isotopes were measured simultaneously by detecting C2 secondary molecular ions, using the on-axis electron multiplier for $^{13}C^{12}C$ and off-axis electron multiplier for $^{12}C2$. Dynamic magnetic field peak switching was used each cycle to measure the nitrogen isotopes (monocollection) using the on-axis electron multiplier to detect $^{12}C^{14}N$ and $^{12}C^{15}N$ molecular ions. The intensity of the primary Cs^+ ion beam for these analyses ranged between 0.05 and 0.25 nanoampere (nA). Instrumental mass fractionation and biological matrix effects were assessed by using an *Escherichia coli* standard (*E. coli*_07, $n = 10$ individual measurements) and compared with the bulk $\delta^{13}C$ composition of the culture measured by conventional gas source mass spectrometry. In this study, a correction of 2.6‰ was applied to the natural abundance $\delta^{13}C$ values. A correction to the labeled ^{15}N values was not applied in this study as the enrichment from ^{15}N in the incubations far exceeded the natural abundance values for the standard. As such, the fractional abundance ^{15}N measured for the ANME aggregates should be considered as a qualitative estimate (i.e., demonstrating the ability to incorporate N_2, rather than quantitative determination of the amount of N_2 assimilated; see ref. 21).

1. Orphan VJ, *et al.* (2004) Geological, geochemical, and microbiological heterogeneity of the seafloor around methane vents in the Eel River Basin, offshore California. *Chem Geol* 205:265–289.
2. Orphan VJ, *et al.* (2001) Comparative analysis of methane-oxidizing archaea and sulfate- reducing bacteria in anoxic marine sediments. *Appl Environ Microbiol* 67:1922–1934.
3. Delong EF (1992) Archaea in coastal marine environments. *Proc Natl Acad Sci USA* 89:5685–5689.
4. Lane D J (1991) in *Nucleic Acid Techniques in Bacterial Systematics*, eds Stackebrandt E, Goodfellow M (John Wiley and Sons, New York), pp 115–175.
5. Mehta MP, Butterfield DA, Baross JA (2003) Phylogenetic diversity of nitrogenase (*nifH*) genes in deep-sea and hydrotheraml vent environments of the Juan de Fuca Ridge. *Appl Environ Microbiol* 69:960–970.
6. Knittel K, *et al.* (2005) Diversity and distribution of methanotrophic Archaea at cold seeps. *Appl Environ Microbiol* 71:467–479.
7. Ravenschlag K, *et al.* (2000) Community structure, cellular rRNA content, and activity of sulfate-reducing bacteria in marine Arctic sediments. *Appl Environ Microbiol* 66:3592–3602.
8. Loy A, *et al.* (2002) Oligonucleotide microarrays for 16S rRNA gene-based detection of all recognized lineages of sulfate-reducing prokaryotes in the environment. *Appl Environ Microbiol* 68:5064–5081.
9. Boetius A, *et al.* (2000) A marine microbial consortium apparently mediating anaerobic oxidation of methane. *Nature* 407:623–626.
10. Manz W, Eisenbrecher M, Neu TR, Szewzyk U (1998) Abundance and spatial organization of Gram-negative sulfate-reducing bacteria in activated sludge investigated by *in situ* probing with specific 16S rRNA targeted oligonucleotides. *FEMS Microbiol Ecol* 25:43–61.
11. Neef, A (1997) in *Faculty for Biology, Chemistry and Geosciences* (Technical University Munich, Munich, Germany).
12. Manz W, *et al.* (1992) Phylogenetic oligodeoxynucleotide probes for the major subclasses of *Proteobacteria*: Problems and solutions. *System Appl Microbiol* 15:593–600.
13. Pernthaler A, Pernthaler J, Amann R (2004) in *Molecular Microbial Ecology Manual*, eds Kowalchuk G, de Bruijn FJ, Head IM, Akkermans ADL, van Elsas JD (Kluwer Academic, Dordrecht, The Netherlands), pp 711–726.
14. Stoffels M, Ludwig W, Schleifer KH (1999) rRNA probe-based cell fishing of bacteria. *Environ Microbiol* 1:259–271.
15. Huse SM, *et al.* (2007) Accuracy and quality of massively parallel DNA pyrosequencing. *Genome Biol* 8:R143.
16. Huson DH, Auch AF, Qi J, Schuster SC (2007) Bioinformatic analysis of metagenomic data. *Genome Res* 17:377–386.
17. Edwards RA, *et al.* (2006) Using pyrosequencing to shed light on deep mine microbial ecology under extreme hydrogeologic conditions. *BMC Genomics* 7:57.
18. Hallam SJ, *et al.* (2004) Reverse methanogenesis: Testing the hypothesis with environmental genomics. *Science* 305:2004.
19. Widdel F, Boetius A, Rabus, R (2007) in *Prokaryotes*, eds Dworkin M, Falkow S, Rosenberg E, Schleifer K-H., Stackebrandt E (Springer, Berlin), Vol 2, pp 1028–1049.
20. Orphan VJ, *et al.* (2002) Multiple archaeal groups mediate methane oxidation in anoxic cold seep sediments. *Proc Natl Acad Sci USA* 99:7663–7668.
21. Lechene CP, Luyten Y, McMahon G, Distel DL (2007) Quantitative imaging of nitrogen fixation by individual bacteria within animal cells. *Science* 317:1563–1566.

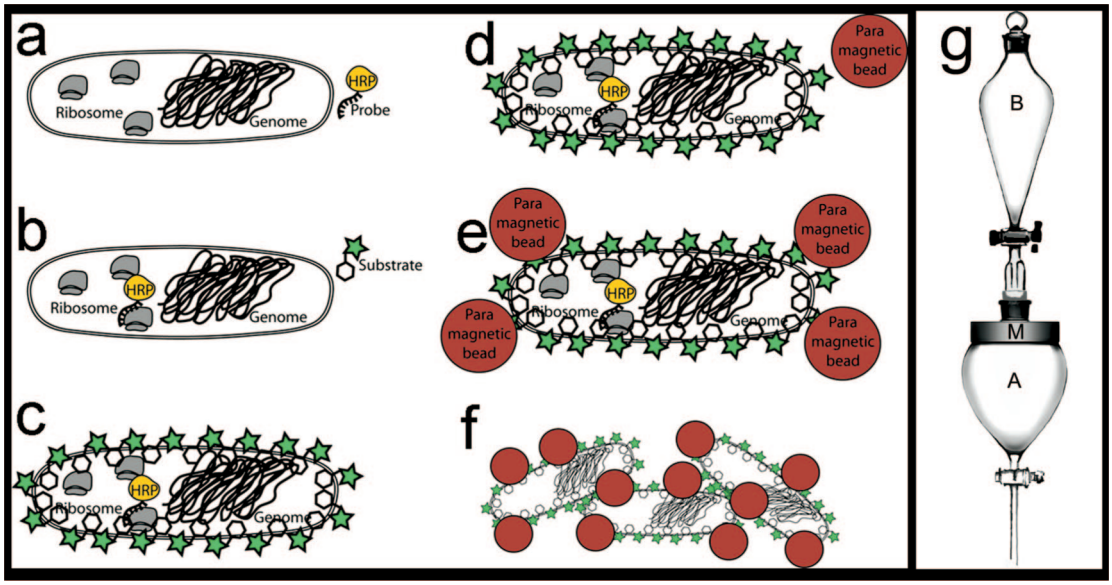

Fig. S1. Schematic drawing of the magneto-FISH procedure. (*a*) hybridization of target cells with a horseradish peroxidase (HRP) labeled oligonucleotide probe. (*b* and *c*) Intracellular deposition of fluorescein labeled tyramide molecules catalyzed by HRP. During the CARD-FISH procedure, fluorescein molecules bound to cellular proteins partially or fully protrude outside of the cell. (*d*) Addition of anti-fluorescein coated paramagnetic beads to hybridized sediment suspension. (*e*) Binding of anti-fluorescein coated beads to fluorescein labeled target cells. (*f*) Magnetic separation of labeled target cells bound to the paramagnetic beads from unlabeled microorganisms and contaminating sediments. (*g*) Apparatus for paramagnetic bead capture. Funnel A contains the hybridized sample and paramagnetic beads suspended in 1× PBS. Ring magnet (M) is seated around the neck of funnel A to concentrate paramagnetic beads and captured cells. Funnel B functions as a reservoir for controlled washing of the magnetically captured sample.

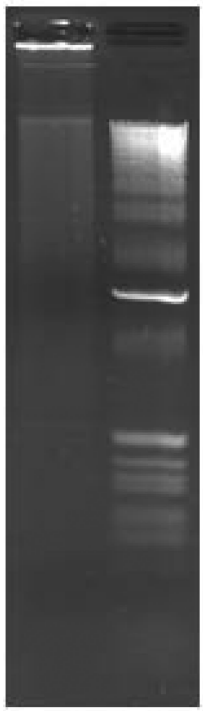

Fig. S2. ANME-2c DNA after multiple displacement amplification (*Left*), and DNA ladder (*Right*). The largest band of the ladder represents 12 kb.

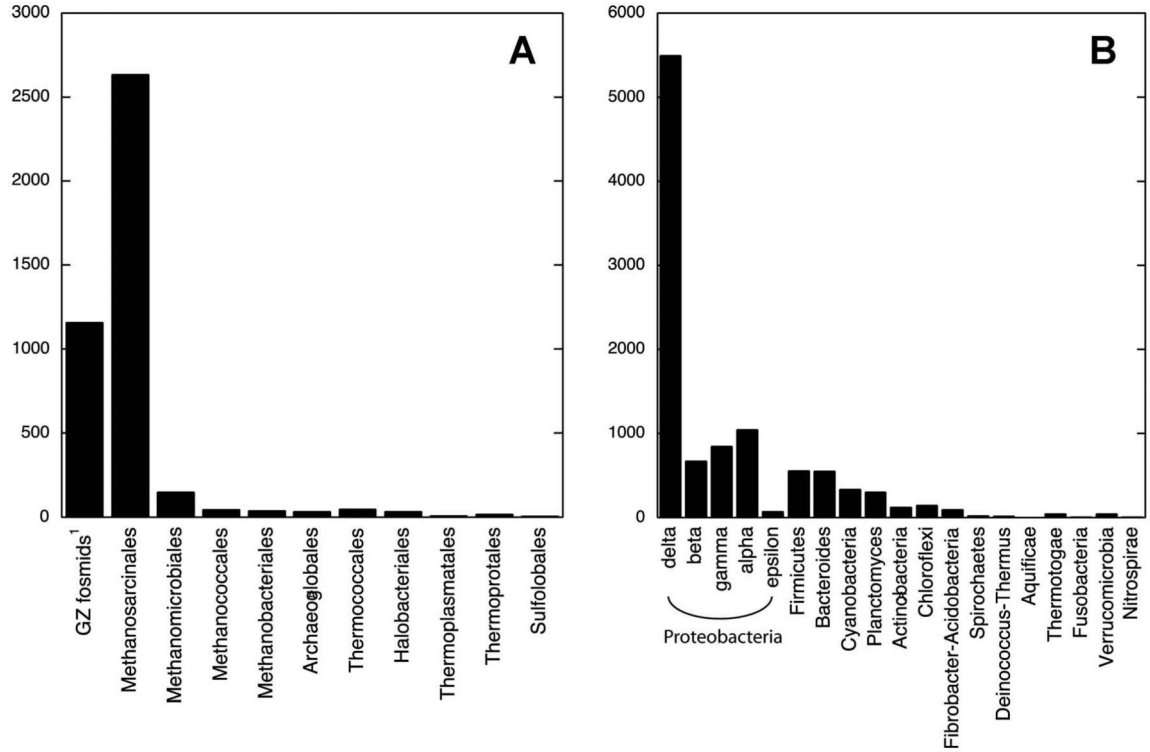

Fig. S3. Taxonomic distribution of identified protein coding 454 reads (39,000 total), from the captured ANME-2c metagenome, classified by using MEGAN style analysis (16) based on closest homologous hit for Archaea (*A*) and Bacteria (*B*).

[1]GZ fosmids from Hallam SJ, *et al*. (2004) Reverse methanogenesis: Testing the hypothesis with environmental genomics. *Science* 305:2004.

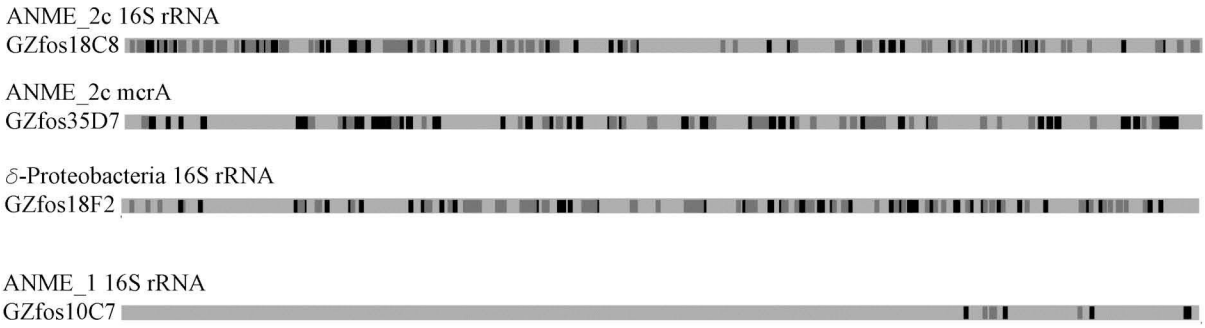

Assigned taxonomic group	Eel River Basin fosmid ID[1]	fosmid length (bp)	Percent coverage
ANME-2	GZfos18C8	39495	30.7
ANME-2	GZfos35D7	25161	35.3
ANME-2	GZfos27A8	38133	34.3
ANME-2	GZfos26B2	25119	24.6
ANME-2	GZfos31B6	34272	24.4
ANME-1	GZfos10C7	36996	2.2
ANME-1	GZfos34H10	29777	2.9
δ-proteobacteria	GZfos18F2	41104	38.8

[1]Hallam et al,. (2004)

Fig. S4. Pyrosequencing coverage estimated with published fosmid clones constructed from Eel River Basin methane seep sediment [Hallam SJ, *et al*. (2004) Reverse methanogenesis: Testing the hypothesis with environmental genomics. *Science* 305:2004. Shading represents degree of regional coverage from light (1× coverage to dark (>1×).

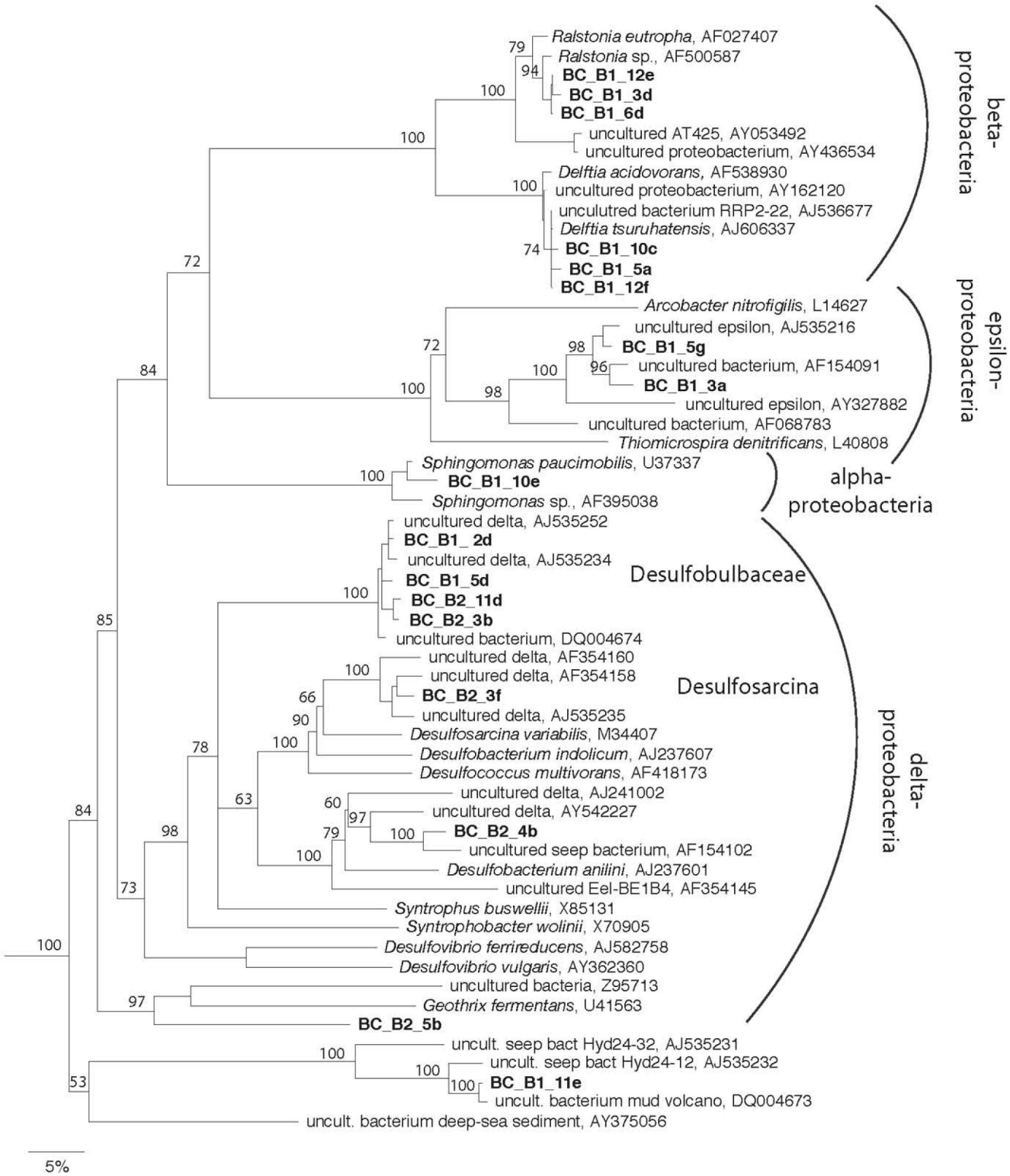

Fig. S5. Phylogenetic relationships of bacteria associated with the magneto-FISH captured ANME-2c consortia, based on sequence divergences within an 1,116-bp region of the 16S rRNA gene, to selected cultured and environmental sequences in public databases. *Thermotoga maritima* (M21774) and *Hydrogenobacter subterraneus* (AB026268) were used as outgroups (data not shown). Numbers next to nodes correspond to bootstrap values based on neighbor-joining distance (5,000 resamplings). GenBank accession numbers for sequences obtained in this study are EU622281–EU622312.

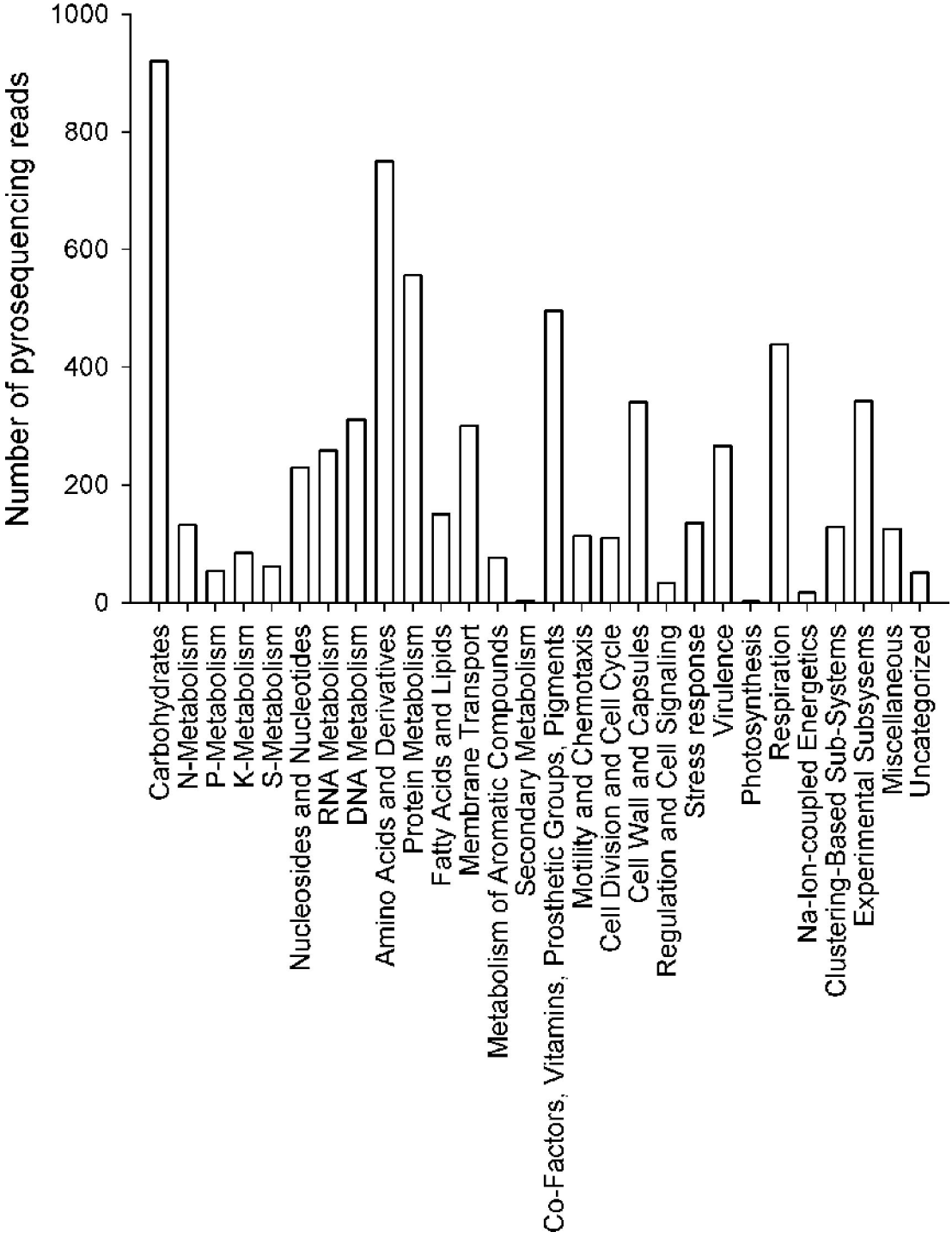

Fig. S6. Subsystems categorization of protein coding 454 reads from the metagenome of the ANME-2c consortium calculated by using the SEED database [Edwards RA, *et al.* (2006) Using pyrosequencing to shed light on deep mine microbial ecology under extreme hydrogeologic conditions. *BMC Genomics* 7:57].

Table S1. Results from reciprocal blast analysis of the pyrosequencing reads against completed genomes from related taxa

Organism	Orthologs, %	Homologs, %	Total
Archaea (Euryarchaeota)			
Methanococcoides burtonii DSM6242	63	64	2,273
Methanosarcina acetivorans	46	52	4,540
Methanococcus vannielii SB	42	42	1,678
Archaeoglobus fulgidus	39	40	2,420
Bacteria (Proteobacteria)			
Delta subgroup			
Desulfotalea psychrophila LSv54	44	46	3,234
Syntrophus aciditrophicus SB	46	48	3,168
Syntrophobacter fumaroxidans MPOB	47	50	4,064
Desulfovibrio vulgaris	37	39	3,531
Beta subgroup			
Ralstonia eutropha H16	28	33	6,206
Burkholderia vietnamiensis G4	24	26	7,617
Alpha subgroup			
Sphingopyxis alaskensis RB2256	34	35	3,195
Gamma subgroup			
Pseudomonas putida KT2440	28	31	5,350
Epsilon subgroup			
Thiomicrospira_denitrificans	34	36	2,097

Table S2. Methanogenesis genes identified in the ANME-2c consortia

Step	Enzyme name	Locus	NCBI accession no.*	Organism	No. of reads†
1	Formylmethanofuran dehydrogenase‡, Subunit A	*fmd/fwbA*	NP_615279.1	*Methanosarcina acetivorans*	6, *1*
	Subunit B	*fmd/fwbB*	NP_615282.1	*Methanosarcina acetivorans*	6, *8*
	Subunit C	*fmd/fwbC*	NP_615280.1	*Methanosarcina acetivorans*	*13*
	Subunit D	*fmd/fwbD*	NP_615281.1	*Methanosarcina acetivorans*	1, *4*
	Subunit E	*fmd/fwbE*	AAU82431.1	Uncultured archaeon GZfos17F1	*3*
	Subunit F	*fmd//fwbF*	NP_615278.1	*Methanosarcina acetivorans*	1, *2*
	Subunit G	*fmd/fwbG*	YP_306396.1	*Methanosarcina barkeri* str. *fusaro*	2, *1*
	Subunit H	*fmd/fwbH*		Missing	
2	Formylmethanofurantetrahydro methanopterin formyltransferase	*ftr*	NP_071032.1	*Archaeoglobus fulgidus*	3, *11*
3	*N*5,*N*10-methenyltetrahydro methanopterin cyclohydrolase	*mch*	AAU82750.1	Uncultured archaeon GZfos19C8	10, *9*
4	F_{420} dependent methylenetetrahydro methanopterin dehydrogenase	*mtd hmd*	YP_565622.1	*Methanococcoides burtonii*	*3*
	5,10-methenyltetrahydro methanopterin hydrogenase.			Missing	—
5	F420-dependent *N*5,*N*10-methenyltetra hydromethanopterin reductase	*mer*	YP_566974.1	*Methanococcoides burtonii*	2, *2*
6	*N*5-methyltetrahydromethanopterin-co-enzyme M methyltransferase, Subunit A	*mtrA*	YP_305584.1	*Methanosarcina barkeri* str. *fusaro*	*1*
	Subunits BCEFG	*mtrBCEFG*		Missing	
	Subunit D	*mtrD*	NP_615248.1	*Methanosarcina acetivorans*	*3*
	Subunit H	*mtrH*	YP_566175.1	*Methanococcoides burtonii*	*3*
7	Methyl coenzyme M reductase, Subunit A	*mcrA*	AAQ63481.1	Uncultured archaeon	2
	Subunit B	*mcrB*	AAQ63477.1	Uncultured archaeon	2, *1*
	Subunit C	*mcrC*	CAJ37202.1	Uncultured methanogenic archaeon RC-I	1
	Subunit D	*mcrD*	AAU83237.1	Uncultured archaeon GZfos27A8	1
	Subunit G	*mcrG*	AAQ63480.1	Uncultured archaeon	1
	Component A2	*mcrA2*	NP_632968.1	*Methanosarcina mazei*	1, *1*
	Heterodisulfide reductase, Subunit A	*hdrA*	AAU82620.1	Uncultured archaeon GZfos18F2	6, *11*
	Subunit B	*hdrB*	CAI64335.1	Uncultured archaeon	4, *1*
	Subunit C	*hdrC*	AAU82747.1	Uncultured archaeon GZfos19C8	*8*
	Subunit D	*hdrD*	NP_615648.1	*Methanosarcina acetivorans*	*7*
	Subunit E	*hdrE*	NP_069495.1	*Archaeoglobus fulgidus*	*2*
	CO dehydrogenase/acetyl-CoA synthase, Subunit A	*cdhA*	AAU82186.1	Uncultured archaeon GZfos11A10	6, *2*
	Subunit B	*cdhB*	YP_565561.1	*Methanococcoides burtonii*	6, *8*
	Subunit C	*cdhC*	AAU82436.1	Uncultured archaeon GZfos17F1	3, *2*
	Subunit D	*cdhD*	YP_565563.1	*Methanococcoides burtonii*	5, *10*
	Subunit E	*cdhE*	YP_502162.1	*Methanospirillum hungatei*	2
	ADP-forming acetyl-CoA synthetase	*acs*	AAU84026.1	Uncultured archaeon GZfos35D7	13, *8*
	methylamine metabolism protein		NP_617819	*Methanosarcina acetivorans*	0, 1
	methanol dehydrogenase regulatory protein		NP_618041	*Methanosarcina acetivorans*	6, 0
	MoxR-related protein methanol dehydrogensae regulator		AAU84139	Uncultured archaeon GZfos37B2	5, 0

*Only one example is given.
†Number of reads with an expectation value of 10−10 (value on the left) or an expectation value between 10−10 and 10−5 (value on the right).
‡Includes both tungsten and molybdenum formylmethanofuran dehydrogenases

Table S3. Reductive Acetyl CoA CO_2 fixation genes identified in ANME-2c consortia

Step	Enzyme name	Locus	NCBI Accession no.*	Organism	No. of gene IDs†
			Delta-Proteobacterial hits		
1	CO-dehydrogenase/Acetyl CoA synthase complex, Subunit A	*cdhA*		Missing	
	Subunit B	*cdhB*	YP_846678.1	*Syntrophobacter fumaroxidans* MPOB	3
	Subunit C	*cdhC*		Missing	
	Subunit D	*cdhD*		Missing	
	Subunit E	*cdhE*		Missing	
2	Pyruvate:Ferredoxin oxidoreductase Subunit A	*porA*	YP_388131.1	*Desulfovibrio desulfuricans* G20	5, *8*
	Subunit B	*porB*	YP_356659.1	*Pelobacter carbinolicus* DSM 2380	*3*
	Subunit D	*porD*	ZP_01673992.1	Candidatus *Desulfococcus oleovorans Hxd*3	*1*
	Subunit G	*porG*	YP_460131.1	*Syntrophus aciditrophicus* SB	*1*
1	CO-dehydrogenase/Acetyl CoA synthase complex, Subunit A	*cdhA*	Archaeal hits	Missing	
	Subunit B	*cdhB*	YP_565561.1	*Methanococcoides burtonii* DSM 6242	2
	Subunit C	*cdhC*		Missing	
	Subunit D	*cdhD*	YP_565563.1	*Methanococcoides burtonii* DSM 6242	2, *4*
	Subunit E	*cdhE*		Missing	
2	Pyruvate:Ferredoxin oxidoreductase Subunit A	*porA*	AAU83985.1	Uncultured *Archaeon* GZfos35B7	1, *11*
	Subunit B	*porB*	AAU83986.1	Uncultured *Archaeon* GZfos35B7	1
	Subunit D	*porD*	YP_001029967	*Methanocorpusculum labreanum* Z	*2*
	Subunit G	*porG*	NP_633366.1	*Methanosarcina mazei* Gö1	*5*

*Only one example is given.
†Number of reads with expectation value of 10−10 (value on the left) or an expectation value between 10−10 and 10−5 (value on the right).

Table S4. Bacterial dissimilatory nitrate reduction genes

Step	Enzyme name	Locus	NCBI accession no. *	Organism	No. of reads†
1	Membrane-bound nitrate reductase (respiratory) alpha subunit	*narG*	YP_001020903	Methylibium petroleiphilum PM1 (β)	*5, 2*
	Nitrate reductase beta subunit	*narH*	YP_524036	Rhodoferax ferrireducens T118 (β)	*1, 1*
	Nitrate reductase gamma subunit	*narI*	ZP_01291344	δ-proteobacterium MLMS-1 (δ)	*2, 7*
	transmembrane nitrate/nitrite sensor kinase	*narQ*	YP_001020884	Methylibium petroleiphilum PM1 (β)	*0, 2*
2	Nitrite reductase	*nirB*	YP_359591	Carboxydothermus hydrogenoformans (Firmicutes)	*0, 1*
	Putative nitrite extrusion protein	*nark*	YP_108904	*Burkholderia pseudomallei* (β)	0, 2
	Signal transduction nitrate/nitrite sensor kinase	*narQ*	YP_523127	Rhodoferax ferrireducens T118 (β)	0, 3
3	Nitric oxide reductase	*norB*	ZP_00946507	*Ralstoniasolanacearum* (β)	2, 0
	Additional subunit of nitric oxide reductase	*norE-like*	YP_286392	Dechloromonas aromatica RCB (β)	0, 1

*Only one example is given.
†Number of reads with an expectation value of 10−10 (value on the left) or an expectation value between 10−10 and 10−5 (value on the right).

Table S5. Nitrogen fixation genes identified in the ANME-2c consortia

Step	Enzyme name	Locus	NCBI accession no.*	Organism	No. of reads†
			Delta-proteobacterial hits		
1	Nitrogenase component 1 Mo-Fe protein, alpha chain	*nifD*	YP_845145.1	*Syntrophobacter fumaroxidans* MPOB	8, 2
	Nitrogenase component 1 Mo-Fe protein, beta chain	*nifK*		N.D.	—
	Nitrogenase component II Fe protein	*nifH*	YP_845148.1	*Syntrophobacter fumaroxidans* MPOB	8
	Nitrogenase Mo-Fe cofactor biosynthesis protein	*nifB*	YP_901617.1	*Pelobacter propionicus* DSM 2379	4, 4
	Nitrogenase Mo-Fe cofactor biosynthesis protein	*nifE*	YP_845142.1	*Syntrophobacter fumaroxidans* MPOB	5
	Nitrogen fixation protein 2Fe-2S-binding	*nifU*	YP_065966.1	*Desulfotalea psychrophila* LSv54	1, 6
	Putative nitrogen fixation protein	*anfA*	YP_064445	*Desulfotalea psychrophila* LSv54	1
	Nitrogen regulatory protein P-II	*glnB*	YP_845146	*Syntrophobacter fumaroxidans* MPOB *Pelobacter propionicus DSM* 2379	10, 14
		glnK	YP_901352		
	ABC-type molybdate transport system			*Syntrophus aciditrophicus* SB	2, 6
			Archaeal hits		
1	Nitrogenase component 1 Mo-Fe protein, alpha chain	*nifD*	P20620	*Methanothermococcus thermolithotrophicus*	1
	Nitrogenase component 1 Mo-Fe protein, beta chain	*nifK*	P51754	*Methanosarcina barkeri*	2
	Nitrogenase Fe protein	*nifH*1	NP_632711	*Methanosarcina mazei* Gö1	1, 3
	Nitrogenase component II Fe protein	*nifH*2	NP_632538	*Methanosarcina mazei* Gö1	1, 3
	Nitrogenase Mo-Fe cofactor biosynthesis protein	*nifB*		N.D.	—
	Nitrogenase Mo-Fe cofactor biosynthesis protein	*nifE*		N.D.	—
	nitrogen-fixing domain protein	*nifU*	YP_843171	*Methanosaeta thermophila* PT	0, 5
	Nitrogen regulatory protein P-II	*glnB*3	P54807	*Methanosarcina barkeri*	0, 3
	Nitrogen regulatory protein P-II	*glnK*	NP_618787	*Methanosarcina acetivorans*	1, 7
			AAU43647	uncultured archaeon GZfos23H7	0, 2
	ABC-type sulfate/molybdate transport systems, ATPase		AAU43644	uncultured archaeon GZfos23H7	3, 20

*Only one example is given.
†Number of reads with an expectation value of 10−10 (value on the left) or an expectation value between 10−10 and 10−5 (value on the right).